

# **Bound-preserving high order schemes for hyperbolic equations: survey and recent developments**

**Chi-Wang Shu**

Division of Applied Mathematics  
Brown University

## Outline

- Introduction
- Bound-preserving first order schemes
- Bound-preserving high order schemes
- Another approach: flux correction
- Numerical results
- Conclusions and future work

## Introduction

We are interested in numerically solving hyperbolic conservation laws

$$u_t + \nabla \cdot \mathbf{F}(u) = 0, \quad u(\mathbf{x}, 0) = u_0(\mathbf{x}) \quad (1)$$

or other related hyperbolic or convection dominated equations. In particular, we are interested in the bound-preserving properties of high order numerical schemes.

We assume the exact solution of the PDE (1) has a **convex** invariant region  $G$ :

- If  $u(\cdot, 0) \in G$ , then  $u(\cdot, t) \in G$  for all  $t > 0$ .

For a convex region  $G$ , if  $u_1, \dots, u_m \in G$ ,  $\alpha_i \geq 0$ ,  $\sum_{i=1}^m \alpha_i = 1$ , then  $u = \sum_{i=1}^m \alpha_i u_i \in G$ . We will heavily use this property when building our high order bound-preserving schemes.

Several examples:

- If (1) is a scalar conservation law, an important property of the entropy solution (which may be discontinuous) is that it satisfies a strict maximum principle: If

$$M = \max_{\mathbf{x}} u_0(\mathbf{x}), \quad m = \min_{\mathbf{x}} u_0(\mathbf{x}), \quad (2)$$

then  $u(\mathbf{x}, t) \in [m, M]$  for any  $\mathbf{x}$  and  $t$ .

Therefore,  $G = [m, M]$  is an invariant region. It is clearly convex.

- For the compressible Euler equations:

$$u_t + f(u)_x = 0$$

with

$$u = \begin{pmatrix} \rho \\ \rho v \\ E \end{pmatrix}, \quad f(u) = \begin{pmatrix} \rho v \\ \rho v^2 + p \\ v(E + p) \end{pmatrix},$$

where  $E = e + \frac{1}{2}\rho v^2$ . The internal energy  $e$  is related to density and pressure through the [equation of states \(EOS\)](#). For the ideal gas, we have  $e = \frac{p}{\gamma-1}$  with  $\gamma = 1.4$  for air.

In this case, we can verify that the set

$$G = \{u : \rho \geq 0, e \geq 0\} \quad (3)$$

is invariant. It is also easy to check that  $G$  is convex (for this we need to check that the internal energy  $e$  is a concave function of the conservative variable  $u$ , then Jensen's inequality implies the convexity of  $G$ ).

For many EOS, e.g. that for the ideal gas, the region  $G$  defined in (3) is equivalent to

$$G = \{u : \rho \geq 0, p \geq 0\}.$$

- Consider the relativistic hydrodynamics

$$u_t + f(u)_x = 0$$

with

$$u = \begin{pmatrix} D \\ m \\ E \end{pmatrix}, f(u) = \begin{pmatrix} Dv \\ mv + p \\ m \end{pmatrix}$$

where  $p$ ,  $D$ ,  $m$  and  $E$  are the thermal pressure, mass density, momentum and energy, respectively.  $v$  is the velocity. Moreover, units are normalized such that the speed of light is  $c = 1$ .

If we denote  $\rho$  to be the proper rest-mass density, then the conservative variable  $u$  can be written as

$$D = \gamma\rho,$$

$$m = Dh\gamma v,$$

$$E = Dh\gamma - p,$$

where  $\gamma = (1 - v^2)^{-1/2}$  is the Lorentz factor and  $h$  is the specific enthalpy. To close the system, we specify an equation of state  $h = h(p, \rho)$ . For ideal gas

$$\rho h = \rho + p\Gamma/(\Gamma - 1)$$

with  $\Gamma$  being the specific heat ratio, such that  $1 < \Gamma \leq 2$



It can be shown that the density  $D$  and pressure  $p$  are positive, and the velocity satisfies  $v^2 \leq 1$ , if they are initially in these cases.

Therefore,

$$G = \{u : D > 0, E > 0, p > 0, v^2 \leq 1\}$$

is an invariant region. It is convex and can be represented as

$$G = \{\mathbf{w} : D > 0, E > \sqrt{D^2 + m^2}\}.$$

Wu and Tang, JCP 2015 and Qin, Shu and Yang, JCP 2016.

## Bound-preserving first order schemes

It is of course desirable to have the invariant region  $G$  also to be an invariant region for the numerical solution. That is, we wish that, if the initial condition  $u(\cdot, 0) \in G$  then  $u(\cdot, t) \in G$  for later time  $t > 0$ . This time  $u$  stands for the numerical solution.

We first consider fulfilling this task for first order schemes.

- First order monotone schemes can easily maintain the maximum principle. For the one-dimensional conservation law

$$u_t + f(u)_x = 0,$$

the first order monotone scheme

$$\begin{aligned} u_j^{n+1} &= H_\lambda(u_{j-1}^n, u_j^n, u_{j+1}^n) \\ &= u_j^n - \lambda[h(u_j^n, u_{j+1}^n) - h(u_{j-1}^n, u_j^n)] \end{aligned}$$

where  $\lambda = \frac{\Delta t}{\Delta x}$  and  $h(u^-, u^+)$  is a monotone flux ( $h(\uparrow, \downarrow)$ ), satisfies

$$H_\lambda(\uparrow, \uparrow, \uparrow)$$

under a suitable CFL condition

$$\lambda \leq \lambda_0.$$

Also, for any constant  $c$ ,

$$H_\lambda(c, c, c) = c - \lambda[h(c, c) - h(c, c)] = c.$$

Therefore, if

$$m \leq u_{j-1}^n, u_j^n, u_{j+1}^n \leq M$$

then

$$u_j^{n+1} = H_\lambda(u_{j-1}^n, u_j^n, u_{j+1}^n) \geq H_\lambda(m, m, m) = m,$$

and

$$u_j^{n+1} = H_\lambda(u_{j-1}^n, u_j^n, u_{j+1}^n) \leq H_\lambda(M, M, M) = M.$$

- For compressible Euler equations, there are several first order schemes, including the Godunov scheme, Lax-Friedrichs scheme, kinetic scheme, HLLC scheme, etc., which satisfy the bound-preserving property for positive density and internal energy (or positive density and pressure for certain EOS), under suitable CFL condition

$$\lambda \leq \lambda_0.$$

- For relativistic hydrodynamics, the first order Lax-Friedrichs scheme is bound-preserving for the invariant region  $G$  mentioned above, under suitable CFL condition

$$\lambda \leq \lambda_0.$$

Wu and Tang, JCP 2015 and Qin, Shu and Yang, JCP 2016.

- For multi-dimensional ideal magnetohydrodynamics (MHD) equations (the symmetrizable version by Godunov), the first order Lax-Friedrichs type scheme is bound-preserving for the invariant region  $G$  with positive density and pressure, under suitable CFL condition

$$\lambda \leq \lambda_0.$$

Wu and Shu, SISC to appear.

We emphasize that it is already non-trivial to find first order schemes which are bound-preserving, e.g. for MHD equations. Since our high order bound-preserving schemes discussed later are built upon first order bound-preserving schemes, the very first task when one would like to solve a new PDE is to find a first order bound-preserving scheme.

**Bound-preserving high order schemes**

For higher order **linear** schemes, i.e. schemes which are linear for a linear PDE

$$u_t + au_x = 0 \quad (4)$$

for example the second order accurate Lax-Wendroff scheme

$$u_j^{n+1} = \frac{a\lambda}{2}(1 + a\lambda)u_{j-1}^n + (1 - a^2\lambda^2)u_j^n - \frac{a\lambda}{2}(1 - a\lambda)u_{j+1}^n$$

where  $\lambda = \frac{\Delta t}{\Delta x}$  and  $|a|\lambda \leq 1$ , the maximum principle is **not** satisfied. In fact, no linear schemes with order of accuracy higher than one can satisfy the maximum principle (Godunov Theorem).

Therefore, nonlinear schemes, namely schemes which are nonlinear even for linear PDEs, have been designed to overcome this difficulty. These include roughly two classes of schemes:

- **TVD schemes.** Most TVD (total variation diminishing) schemes also satisfy strict maximum principle, even in multi-dimensions. TVD schemes can be designed for any formal order of accuracy **for solutions in smooth, monotone regions**. However, **all** TVD schemes will degenerate to first order accuracy at smooth extrema.
- **TVB schemes, ENO schemes, WENO schemes.** These schemes do not insist on strict TVD properties, therefore they do **not** satisfy strict maximum principles, although they can be designed to be arbitrarily high order accurate for smooth solutions.



A high order finite volume scheme has the following algorithm flowchart:

- (1) Given  $\{\bar{u}_j^n\}$
- (2) reconstruct  $u^n(x)$  (piecewise polynomial with cell average  $\bar{u}_j^n$ )
- (3) evolve by, e.g. Runge-Kutta time discretization to get  $\{\bar{u}_j^{n+1}\}$
- (4) return to (1)

A high order discontinuous Galerkin scheme has a similar algorithm flowchart:

- (1) Given  $u^n(x)$  (piecewise polynomial with the cell average  $\bar{u}_j^n$ )
- (2) evolve by, e.g. Runge-Kutta time discretization to get  $u^{n+1}(x)$   
(with the cell average  $\{\bar{u}_j^{n+1}\}$ )
- (3) return to (1)

We will call a finite volume or DG scheme bound-preserving, if we have

$$m \leq u^{n+1}(x) \leq M, \quad \forall x$$

provided

$$m \leq u^n(x) \leq M, \quad \forall x.$$

A suitable modification to evaluate the bounds only at certain quadrature points will be given later to facilitate easy implementation.

The flowchart for designing a high order finite volume or DG scheme which obeys a strict maximum principle is as follows:

1. Start with  $u^n(x)$  which is high order accurate

$$|u(x, t^n) - u^n(x)| \leq C \Delta x^p$$

and satisfies

$$m \leq u^n(x) \leq M, \quad \forall x$$

therefore of course we also have

$$m \leq \bar{u}_j^n \leq M, \quad \forall j.$$

2. Evolve for one time step to get

$$m \leq \bar{u}_j^{n+1} \leq M, \quad \forall j. \quad (5)$$

3. Given (5) above, obtain  $u^{n+1}(x)$  (reconstruction or evolution) which

- satisfies the maximum principle

$$m \leq u^{n+1}(x) \leq M, \quad \forall x;$$

- is high order accurate

$$|u(x, t^{n+1}) - u^{n+1}(x)| \leq C \Delta x^p.$$

Three major difficulties

1. **The first difficulty is** how to evolve in time for one time step to guarantee

$$m \leq \bar{u}_j^{n+1} \leq M, \quad \forall j. \quad (6)$$

**This is very difficult to achieve.** Previous works use one of the following two approaches:

- Use exact time evolution. This can guarantee

$$m \leq \bar{u}_j^{n+1} \leq M, \quad \forall j.$$

However, it can only be implemented with reasonable cost for linear PDEs, or for nonlinear PDEs in one dimension. This approach was used in, e.g., [Jiang and Tadmor, SISC 1998](#); [Liu and Osher, SINUM 1996](#); [Sanders, Math Comp 1988](#); [Qiu and Shu, SINUM 2008](#); [Zhang and Shu, SINUM 2010](#); to obtain TVD schemes or maximum-principle-preserving schemes for linear and nonlinear PDEs in one dimension or for linear PDEs in multi-dimensions, for second or third order accurate schemes.

- Use simple time evolution such as SSP Runge-Kutta or multi-step methods. However, additional limiting will be needed on  $u^n(x)$  which will destroy accuracy near smooth extrema.

In [Zhang and Shu, JCP 2010a](#), a procedure is designed to obtain

$$m \leq \bar{u}_j^{n+1} \leq M, \quad \forall j$$

with simple Euler forward or SSP Runge-Kutta or multi-step methods without losing accuracy on the limited  $u^n(x)$ :



The evolution of the cell average for a higher order finite volume or DG scheme satisfies

$$\begin{aligned}\bar{u}_j^{n+1} &= G(\bar{u}_j^n, u_{j-\frac{1}{2}}^-, \textcolor{blue}{u}_{j-\frac{1}{2}}^+, \textcolor{blue}{u}_{j+\frac{1}{2}}^-, u_{j+\frac{1}{2}}^+) \\ &= \bar{u}_j^n - \lambda[h(u_{j+\frac{1}{2}}^-, u_{j+\frac{1}{2}}^+) - h(u_{j-\frac{1}{2}}^-, u_{j-\frac{1}{2}}^+)],\end{aligned}$$

where

$$G(\uparrow, \uparrow, \textcolor{blue}{\downarrow}, \textcolor{blue}{\downarrow}, \uparrow)$$

therefore there is no maximum principle. The problem is with the two arguments  $u_{j-\frac{1}{2}}^+$  and  $u_{j+\frac{1}{2}}^-$  which are values at points inside the cell  $I_j$ .

The polynomial  $p_j(x)$  (either reconstructed in a finite volume method or evolved in a DG method) is of degree  $k$ , defined on  $I_j$  such that  $\bar{u}_j^n$  is its cell average on  $I_j$ ,  $u_{j-\frac{1}{2}}^+ = p_j(x_{j-\frac{1}{2}})$  and  $u_{j+\frac{1}{2}}^- = p_j(x_{j+\frac{1}{2}})$ .

We take a Legendre Gauss-Lobatto quadrature rule which is exact for polynomials of degree  $k$ , then

$$\bar{u}_j^n = \sum_{\ell=0}^m \omega_\ell p_j(y_\ell)$$

with  $y_0 = x_{j-\frac{1}{2}}$ ,  $y_m = x_{j+\frac{1}{2}}$ . The scheme for the cell average is then rewritten as

$$\begin{aligned}
 \bar{u}_j^{n+1} &= \omega_m \left[ u_{j+\frac{1}{2}}^- - \frac{\lambda}{\omega_m} \left( h(u_{j+\frac{1}{2}}^-, u_{j+\frac{1}{2}}^+) - h(u_{j-\frac{1}{2}}^+, u_{j+\frac{1}{2}}^-) \right) \right] \\
 &\quad + \omega_0 \left[ u_{j-\frac{1}{2}}^+ - \frac{\lambda}{\omega_0} \left( h(u_{j-\frac{1}{2}}^+, u_{j+\frac{1}{2}}^-) - h(u_{j-\frac{1}{2}}^-, u_{j-\frac{1}{2}}^+) \right) \right] \\
 &\quad + \sum_{\ell=1}^{m-1} \omega_\ell p_j(y_\ell) \\
 &= \omega_m H_{\lambda/\omega_m} (u_{j-\frac{1}{2}}^+, u_{j+\frac{1}{2}}^-, u_{j+\frac{1}{2}}^+) + \omega_0 H_{\lambda/\omega_0} (u_{j-\frac{1}{2}}^-, u_{j-\frac{1}{2}}^+, u_{j+\frac{1}{2}}^-) \\
 &\quad + \sum_{\ell=1}^{m-1} \omega_\ell p_j(y_\ell).
 \end{aligned}$$

Therefore, if

$$m \leq p_j(y_\ell) \leq M$$

at all Legendre Gauss-Lobatto quadrature points and a reduced CFL condition

$$\lambda/\omega_m = \lambda/\omega_0 \leq \lambda_0$$

is satisfied, then

$$m \leq \bar{u}_j^{n+1} \leq M.$$

2. The second difficulty is: given

$$m \leq \bar{u}_j^{n+1} \leq M, \quad \forall j$$

how to obtain an **accurate**  $u^{n+1}(x)$  (reconstruction or limited DG evolution) which satisfies

$$m \leq u^{n+1}(x) \leq M, \quad \forall x.$$

Previous work was mainly for relatively lower order schemes (second or third order accurate), and would typically require an evaluation of the extrema of  $u^{n+1}(x)$ , which, for a piecewise polynomial of higher degree, is quite costly.

Again in [Zhang and Shu, JCP 2010a](#), a procedure is designed to obtain such  $u^{n+1}(x)$  with a very simple scaling limiter, which only requires the evaluation of  $u^{n+1}(x)$  at certain pre-determined quadrature points and does not destroy accuracy:

We replace  $p_j(x)$  by the limited polynomial  $\tilde{p}_j(x)$  defined by

$$\tilde{p}_j(x) = \theta_j(p_j(x) - \bar{u}_j^n) + \bar{u}_j^n$$

where

$$\theta_j = \min \left\{ \left| \frac{M - \bar{u}_j^n}{M_j - \bar{u}_j^n} \right|, \left| \frac{m - \bar{u}_j^n}{m_j - \bar{u}_j^n} \right|, 1 \right\},$$

with

$$M_j = \max_{x \in S_j} p_j(x), \quad m_j = \min_{x \in S_j} p_j(x)$$

where  $S_j$  is the set of Legendre Gauss-Lobatto quadrature points of cell  $I_j$ .

Clearly, this limiter is just a simple scaling of the original polynomial around its average.

The following lemma, guaranteeing the maintenance of accuracy of this simple limiter, is proved in [Zhang and Shu, JCP 2010a](#):

**Lemma:** Assume  $\bar{u}_j^n \in [m, M]$  and  $p_j(x)$  is an  $O(\Delta x^p)$  approximation, then  $\tilde{p}_j(x)$  is also an  $O(\Delta x^p)$  approximation.

We have thus obtained a high order accurate scheme satisfying the following maximum principle: If

$$m \leq u^n(x) \leq M, \quad \forall x \in S_j,$$

then

$$m \leq u^{n+1}(x) \leq M, \quad \forall x \in S_j.$$

Recall that  $S_j$  is the set of Legendre Gauss-Lobatto quadrature points of cell  $I_j$ .



3. **The third difficulty is** how to generalize the algorithm and result to 2D (or higher dimensions). Algorithms which would require an evaluation of the extrema of the reconstructed polynomials  $u^{n+1}(x, y)$  would not be easy to generalize at all.

Our algorithm uses only explicit Euler forward or SSP (also called TVD) Runge-Kutta or multi-step time discretizations, and a simple scaling limiter involving just evaluation of the polynomial at certain quadrature points, hence easily generalizes to 2D or higher dimensions on structured or unstructured meshes, with strict maximum-principle-satisfying property and provable high order accuracy.

The technique has been generalized to the following situations maintaining uniformly high order accuracy:

- 2D scalar conservation laws on rectangular or triangular meshes with strict maximum principle (Zhang and Shu, JCP 2010a; Zhang, Xia and Shu, JSC 2012).
- 2D incompressible equations in the vorticity-streamfunction formulation (with strict maximum principle for the vorticity), and 2D passive convections in a divergence-free velocity field, i.e.

$$\omega_t + (u\omega)_x + (v\omega)_y = 0,$$

with a given divergence-free velocity field  $(u, v)$ , again with strict maximum principle (Zhang and Shu, JCP 2010a; Zhang, Xia and Shu, JSC 2012).

- One and multi-dimensional compressible Euler equations maintaining positivity of density and pressure ([Zhang and Shu, JCP 2010b](#); [Zhang, Xia and Shu, JSC 2012](#)).
- One and two-dimensional shallow water equations maintaining non-negativity of water height and well-balancedness for problems with dry areas ([Xing, Zhang and Shu, Advances in Water Resources 2010](#); [Xing and Shu, Advances in Water Resources 2011](#)).
- One and multi-dimensional compressible Euler equations with source terms (geometric, gravity, chemical reaction, radiative cooling) maintaining positivity of density and pressure ([Zhang and Shu, JCP 2011](#)).

- One and multi-dimensional compressible Euler equations with gaseous detonations maintaining positivity of density, pressure and reactant mass fraction, with a new and simplified implementation of the pressure limiter. DG computations are stable without using the TVB limiter ([Wang, Zhang, Shu and Ning, JCP 2012](#)).
- A minimum entropy principle satisfying high order scheme for gas dynamics equations ([Zhang and Shu, Num Math 2012](#)).
- Cosmological hydrodynamical simulation of turbulence in the intergalactic medium (IGM) involving kinetic energy dominated flows ([Zhu, Feng, Xia, Shu, Gu and Fang, Astrophysical J. 2013](#)).
- Ideal special relativistic hydrodynamics (RHD) ([Qin, Shu and Yang, JCP 2016](#)).

- Positivity-preserving high order finite difference WENO schemes for compressible Euler equations ([Zhang and Shu, JCP 2012](#)).
- Simplified version for WENO finite volume schemes without the need to evaluate solutions at quadrature points inside the cell ([Zhang and Shu, Proceedings of the Royal Society A, 2011](#)).
- Positivity-preserving for PDEs involving global integral terms including a hierarchical size-structured population model ([Zhang, Zhang and Shu, JCAM 2011](#)), Vlasov-Boltzmann transport equations ([Cheng, Gamba and Proft, Math Comp 2012](#)), and correlated random walk with density-dependent turning rates ([Lu, Shu and Zhang, Sci. China Math 2013](#)).

- Positivity-preserving semi-Lagrangian schemes ([Qiu and Shu, JCP 2011](#); [Rossmanith and Seal, JCP 2011](#)).
- Positivity-preserving first order and higher order Lagrangian schemes for multi-material flows ([Cheng and Shu, JCP 2014](#); [Vilar, Shu and Maire, JCP 2016a, JCP2016b](#)).
- Implicit time discretization (needs a lower bound for CFL, [Qin and Shu, SISC 2018](#))

- Positivity-preserving DG methods for radiative transfer equations, with iterative procedure for steady states or implicit time discretization for time-dependent equations (Yuan, Cheng and Shu, SISC 2016; Ling, Cheng and Shu, JSC to appear).
- Positivity-preserving DG methods for ideal magnetohydrodynamics (MHD) equations (Cheng, Li, Qiu and Xu, JCP 2013; Wu, SINUM 2018; Wu and Shu, SISC to appear).

**Another approach: flux correction**

Another approach to achieve bound-preserving schemes is through the traditional flux-correction method, namely modify the numerical flux by

$$\hat{f} = \theta \hat{f}^h + (1 - \theta) \hat{f}^l$$

where  $\hat{f}^h$  is the high order numerical flux and  $\hat{f}^l$  is the first order numerical flux (which does lead to a bound-preserving first order scheme).

Many traditional TVD or bound-preserving schemes follow this approach. It is relatively easy to design  $\theta$  to guarantee bound-preserving, but it is relatively more difficult to guarantee accuracy (and often accuracy is lost, especially near smooth extrema).



Recently, this approach has been revived. The limiter in [Hu, Adam and Shu, JCP 2013](#) belongs to this class. We mention in particular the work of Zhengfu Xu (the high order parametrized maximum-principle-preserving and positivity-preserving finite difference schemes, [Xu, Math Comp 2014](#)). This is one of the rare cases that such flux-correction method has been proved to maintain the original high order accuracy even near smooth extrema. However, the proof is via explicit and complicated algebraic verifications, thus limiting the scope that it can be applied. See [Liang and Xu, JSC 2014](#) (scalar conservation law); [Xiong, Qiu and Xu, JCP 2013](#) (incompressible flow); [Christlieb, Liu, Tang and Xu, JCP 2015](#) (unstructured mesh) and [SISC 2015](#) (MHD); [Jiang, Shu and Zhang,  \$M^3AS\$  2015](#) (correlated random walk); [Wu and Tang, JCP 2015](#) (special relativistic hydrodynamics).

## Numerical results

**Example 1.** Accuracy check. For the incompressible Euler equation in the vorticity-streamfunction formulation, with periodic boundary condition and initial data  $\omega(x, y, 0) = -2 \sin(x) \sin(y)$  on the domain  $[0, 2\pi] \times [0, 2\pi]$ , the exact solution is  $\omega(x, y, t) = -2 \sin(x) \sin(y)$ . We clearly observe the designed order of accuracy for this solution.

Table 1: Incompressible Euler equations.  $P^2$  for vorticity,  $t = 0.5$ .

| $N \times N$     | $L^1$ error | order | $L^\infty$ error | order |
|------------------|-------------|-------|------------------|-------|
| $16 \times 16$   | 5.12E-4     | –     | 1.40E-3          | –     |
| $32 \times 32$   | 3.75E-5     | 3.77  | 1.99E-4          | 2.81  |
| $64 \times 64$   | 3.16E-6     | 3.57  | 2.74E-5          | 2.86  |
| $128 \times 128$ | 2.76E-7     | 3.51  | 3.56E-6          | 2.94  |

**Example 2.** The vortex patch problem. We solve the incompressible Euler equations in  $[0, 2\pi] \times [0, 2\pi]$  with the initial condition

$$\omega(x, y, 0) = \begin{cases} -1, & \frac{\pi}{2} \leq x \leq \frac{3\pi}{2}, \frac{\pi}{4} \leq y \leq \frac{3\pi}{4}; \\ 1, & \frac{\pi}{2} \leq x \leq \frac{3\pi}{2}, \frac{5\pi}{4} \leq y \leq \frac{7\pi}{4}; \\ 0, & \text{otherwise} \end{cases}$$

and periodic boundary conditions. The contour plots of the vorticity  $\omega$  are given for  $t = 10$ . Again, we cannot observe any significant difference between the two results in the contour plots. The cut along the diagonal gives us a clearer view of the advantage in using the limiter.

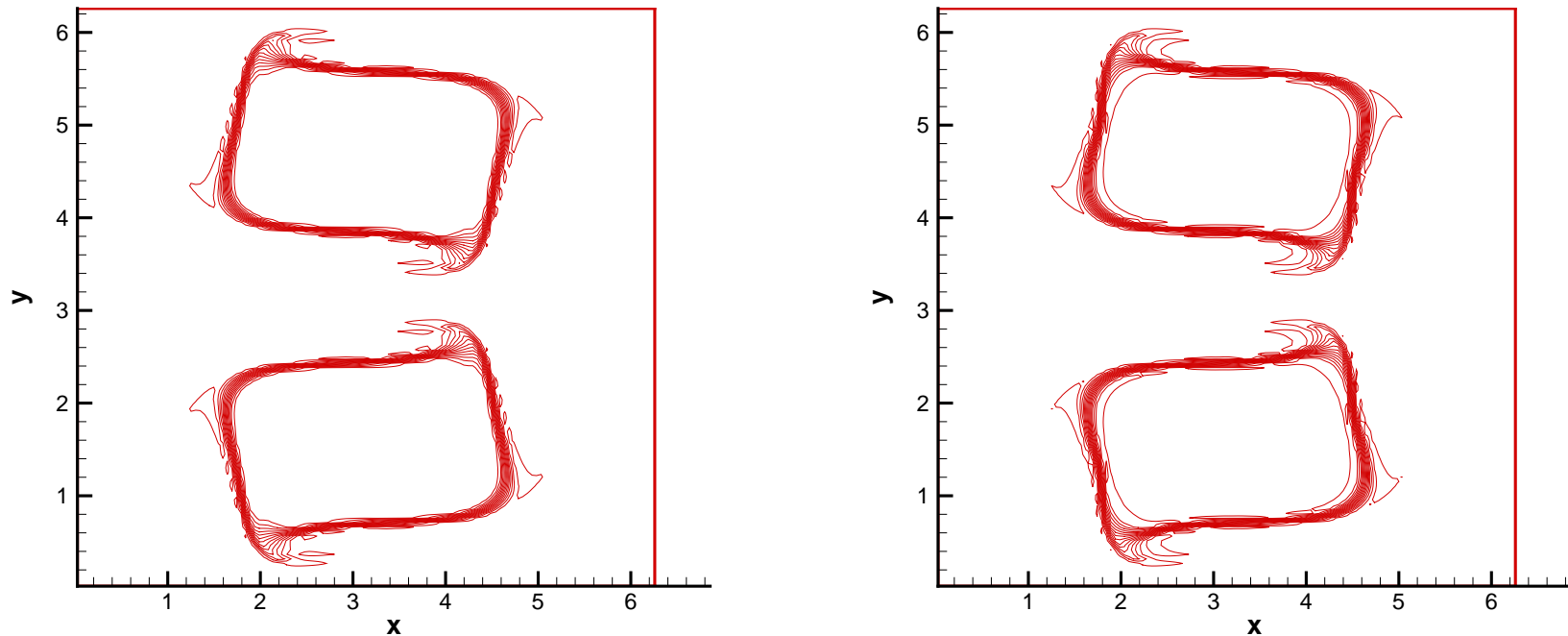


Figure 1: Vorticity at  $t = 10$ ,  $P^2$ . 30 equally spaced contours from  $-1.1$  to  $1.1$ .  $128^2$  mesh. Left: with limiter; Right: without limiter.

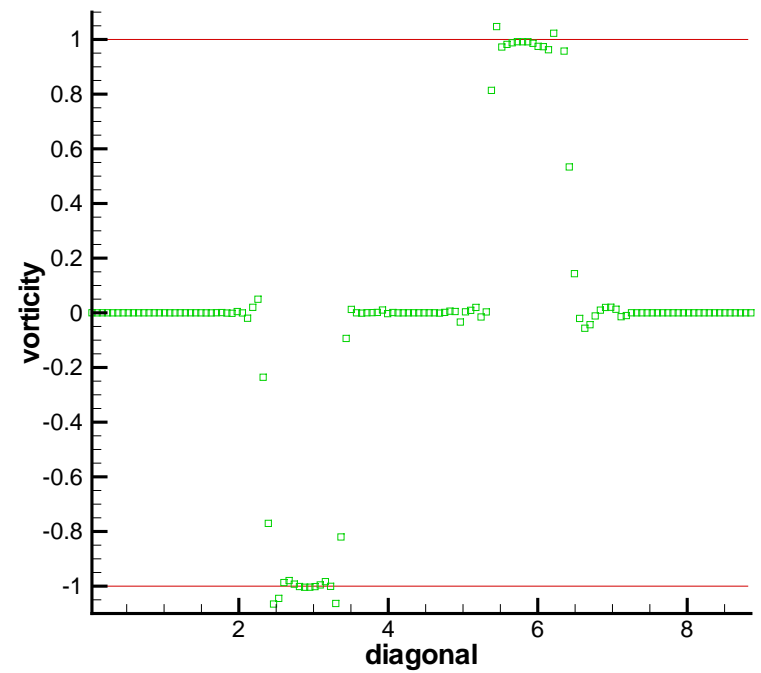
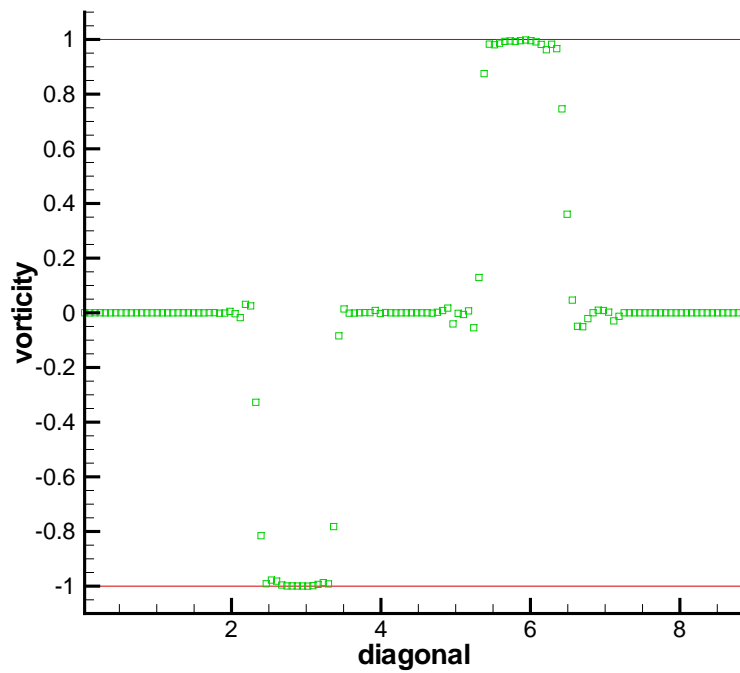


Figure 2: Vorticity at  $t = 10$ ,  $P^2$ . Cut along the diagonal.  $128^2$  mesh. Left: with limiter; Right: without limiter.

**Example 3.** The Sedov point-blast wave in one dimension. For the initial condition, the density is 1, velocity is zero, total energy is  $10^{-12}$  everywhere except that the energy in the center cell is the constant  $\frac{E_0}{\Delta x}$  with  $E_0 = 3200000$  (emulating a  $\delta$ -function at the center).  $\gamma = 1.4$ . The computational results are shown in Figure 3. We can see the shock is captured very well.

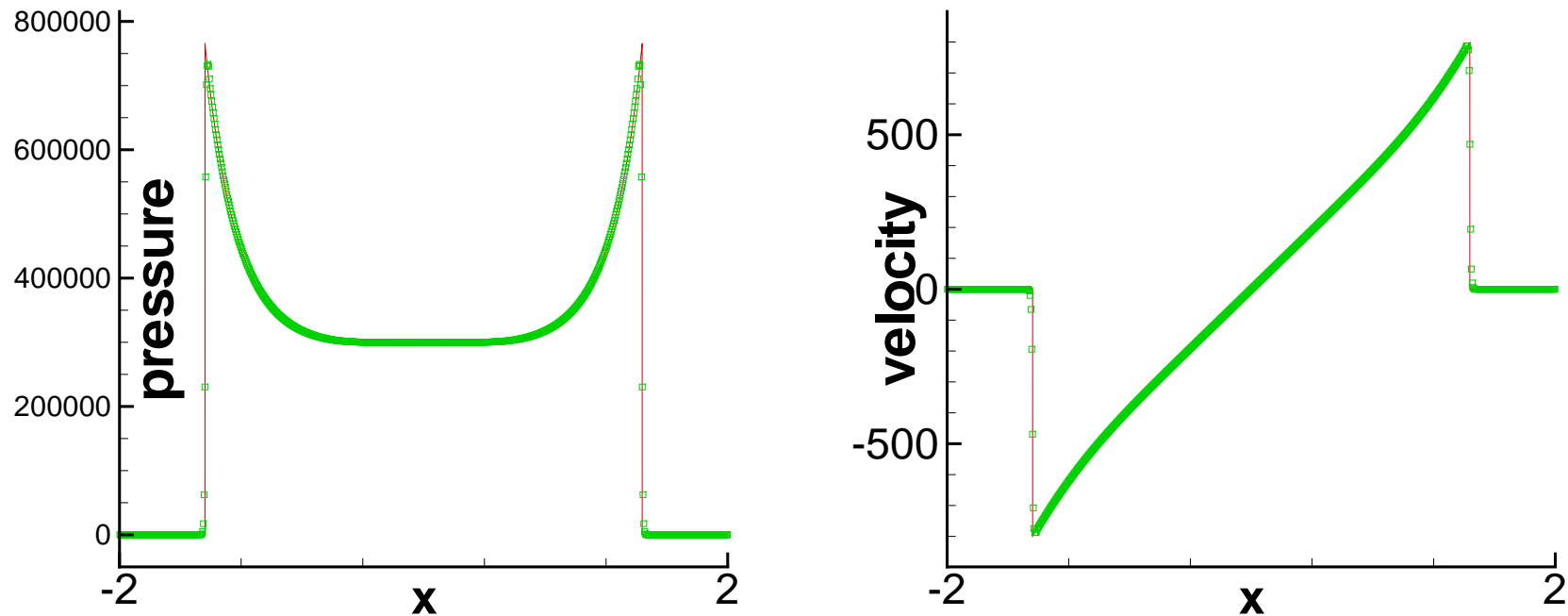


Figure 3: 1D Sedov blast. The solid line is the exact solution. Symbols are numerical solutions.  $T = 0.001$ .  $N = 800$ .  $\Delta x = \frac{4}{N}$ . TVB limiter parameters  $(M_1, M_2, M_3) = (15000, 20000, 15000)$ . Pressure (left) and velocity (right).



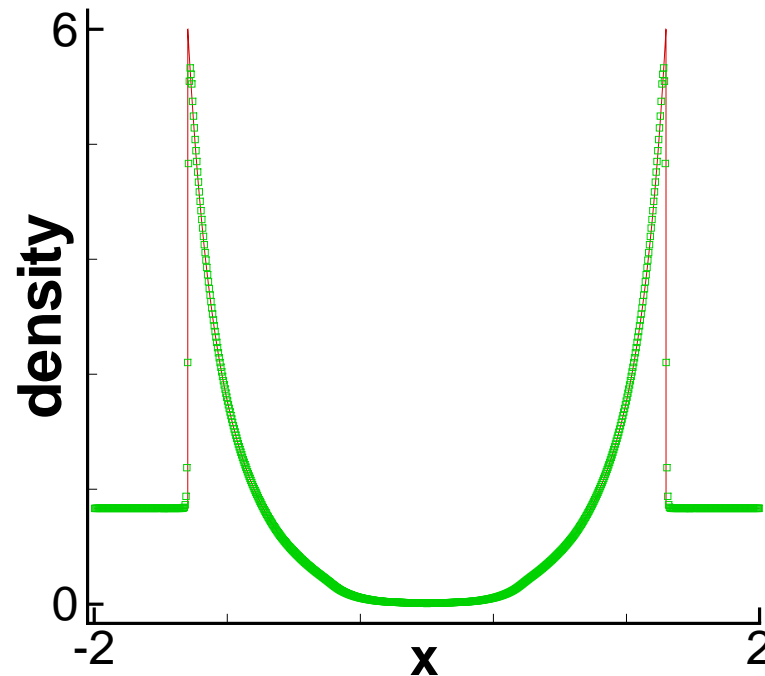


Figure 4: 1D Sedov blast. The solid line is the exact solution. Symbols are numerical solutions.  $T = 0.001$ .  $N = 800$ .  $\Delta x = \frac{4}{N}$ . TVB limiter parameters  $(M_1, M_2, M_3) = (15000, 20000, 15000)$ . Density.

**Example 4.** The Sedov point-blast wave in two dimensions. The computational domain is a square. For the initial condition, the density is 1, velocity is zero, total energy is  $10^{-12}$  everywhere except that the energy in the lower left corner cell is the constant  $\frac{0.244816}{\Delta x \Delta y}$ .  $\gamma = 1.4$ . See Figure 5. The computational result is comparable to those in the literature, e.g. those computed by Lagrangian methods.

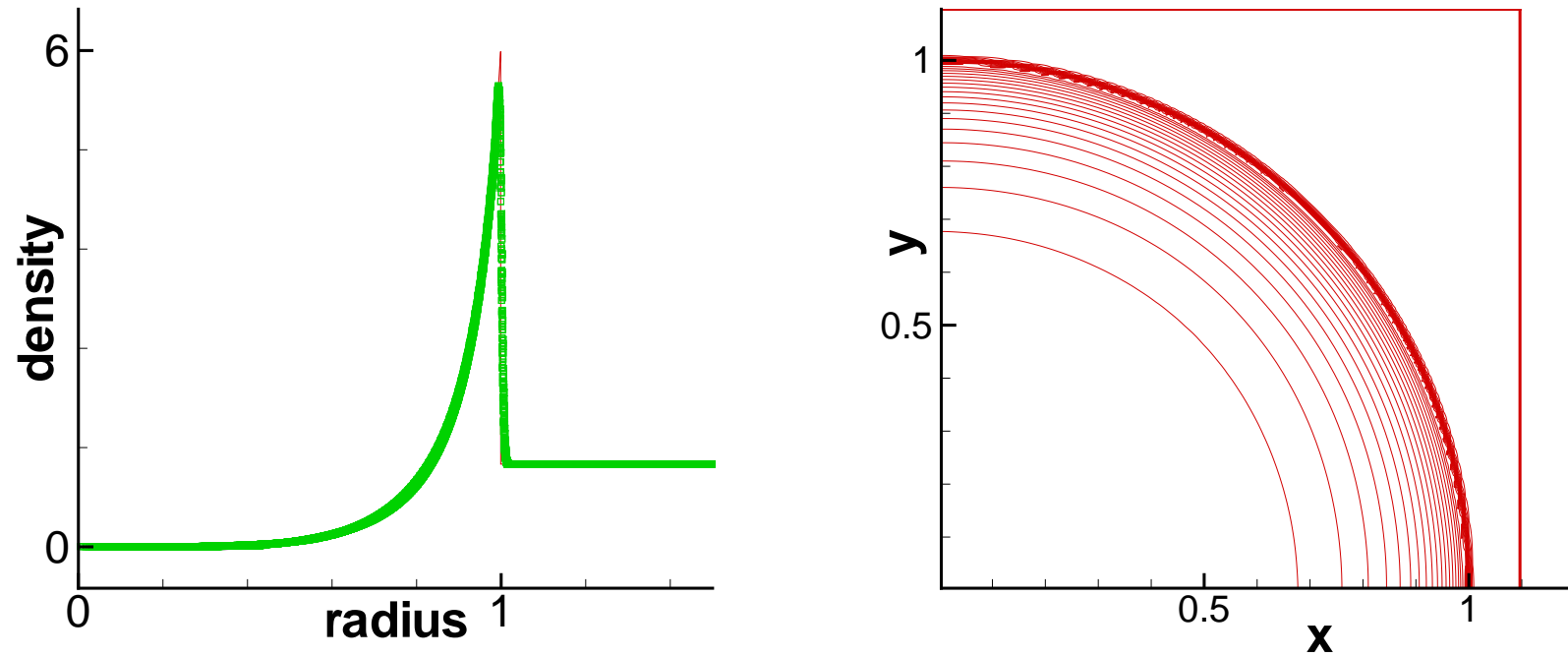


Figure 5: 2D Sedov blast, plot of density.  $T = 1$ .  $N = 160$ .  $\Delta x = \Delta y = \frac{1.1}{N}$ . TVB limiter parameters  $(M_1, M_2, M_3, M_4) = (8000, 16000, 16000, 8000)$ .

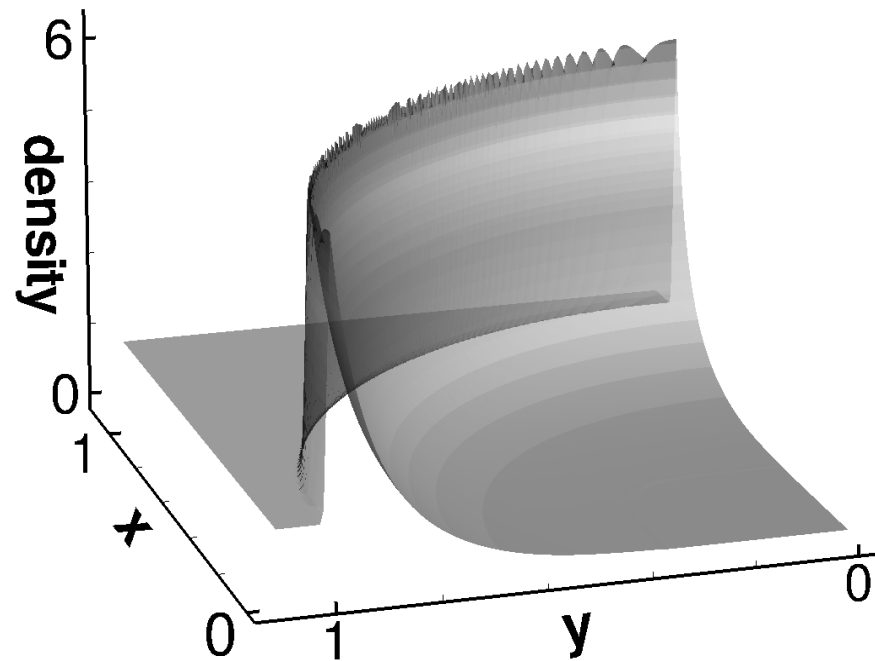


Figure 6: 2D Sedov blast, plot of density.  $T = 1$ .  $N = 160$ .  $\Delta x = \Delta y = \frac{1.1}{N}$ . TVB limiter parameters  $(M_1, M_2, M_3, M_4) = (8000, 16000, 16000, 8000)$ .

**Example 5.** We consider two Riemann problems. The first one is a double rarefaction. We did two tests, one is a one-dimensional double rarefaction, for which the initial condition is  $\rho_L = \rho_R = 7$ ,  $u_L = -1$ ,  $u_R = 1$ ,  $p_L = p_R = 0.2$  and  $\gamma = 1.4$ . The other one is a two-dimensional double rarefaction with the initial condition  $\rho_L = \rho_R = 7$ ,  $u_L = -1$ ,  $u_R = 1$ ,  $v_L = v_R = 0$ ,  $p_L = p_R = 0.2$ . The exact solution contains vacuum.

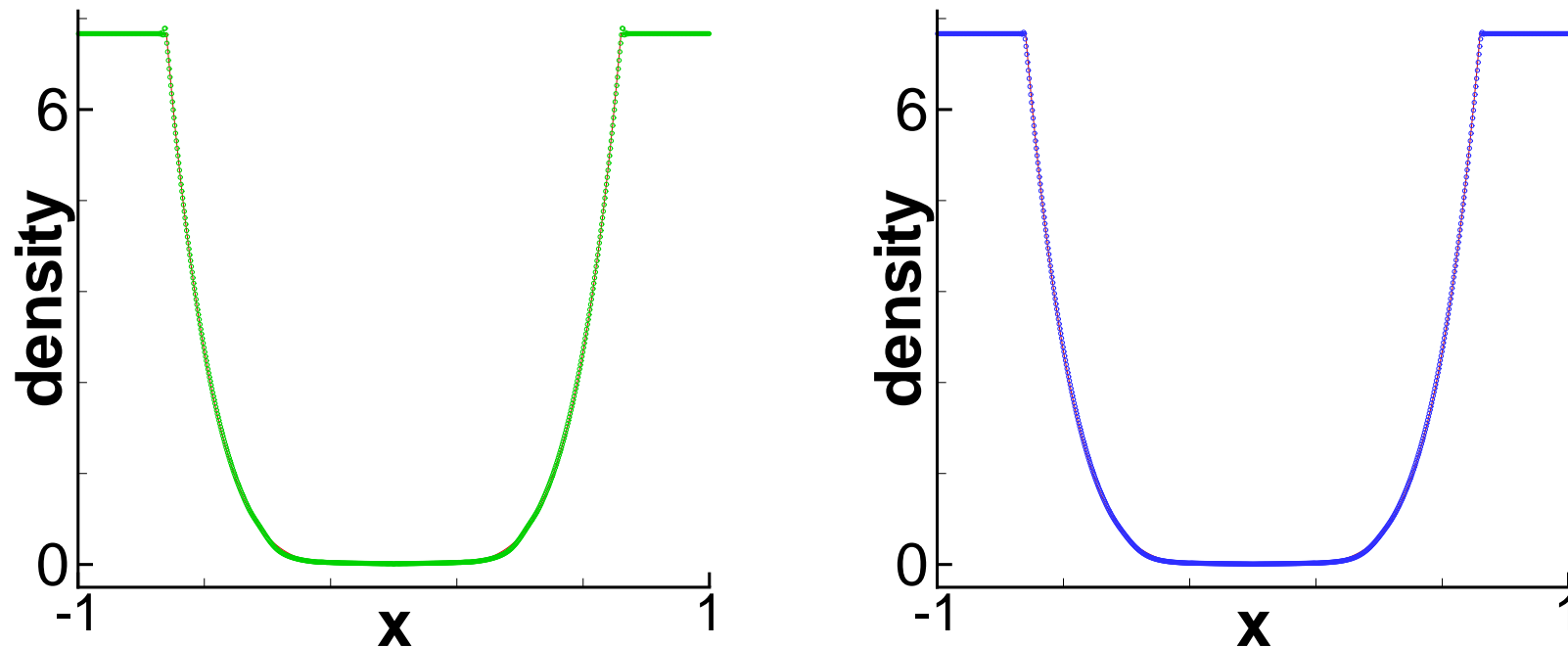


Figure 7: Double rarefaction problem.  $T=0.6$ . Left: 1D problem. Right: Cut at  $y = 0$  for the 2D problem. Every fourth cell is plotted. The solid line is the exact solution. Symbols are numerical solutions.  $\Delta x = \frac{2}{N}$ ,  $N = 800$  with the positivity limiter. Density.

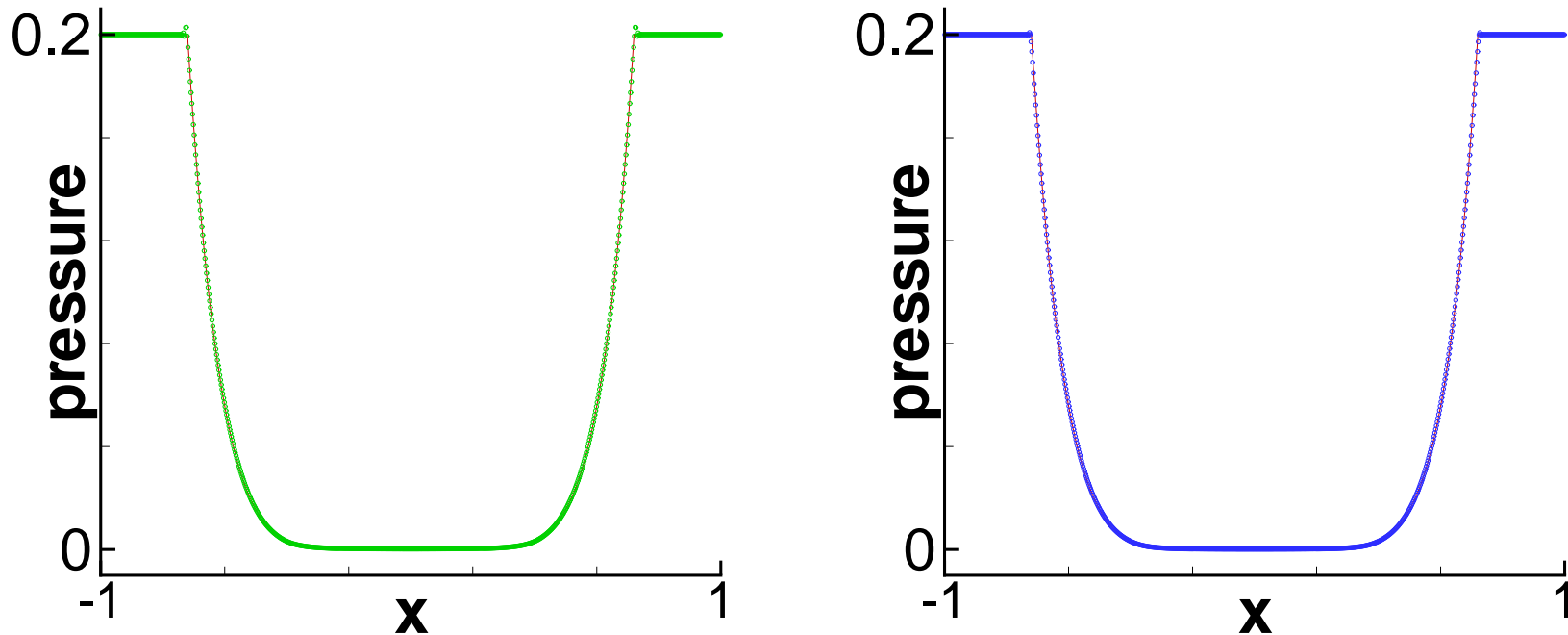


Figure 8: Double rarefaction problem.  $T=0.6$ . Left: 1D problem. Right: Cut at  $y = 0$  for the 2D problem. Every fourth cell is plotted. The solid line is the exact solution. Symbols are numerical solutions.  $\Delta x = \frac{2}{N}$ ,  $N = 800$  with the positivity limiter. Pressure.

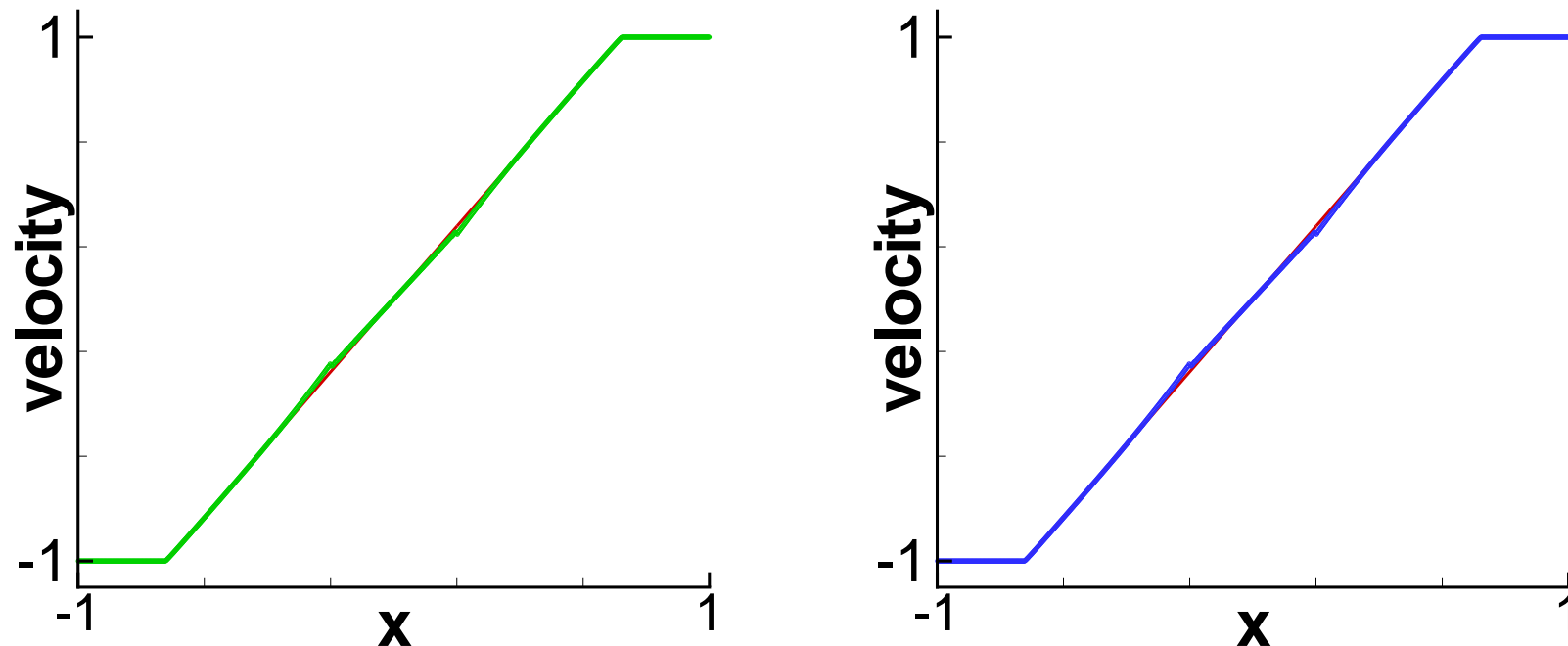


Figure 9: Double rarefaction problem.  $T=0.6$ . Left: 1D problem. Right: Cut at  $y = 0$  for the 2D problem. Every fourth cell is plotted. The solid line is the exact solution. Symbols are numerical solutions.  $\Delta x = \frac{2}{N}$ ,  $N = 800$  with the positivity limiter. Velocity.



The second one is a 1D Leblanc shock tube problem. The initial condition is  $\rho_L = 2$ ,  $\rho_R = 0.001$ ,  $u_L = u_R = 0$ ,  $p_L = 10^9$ ,  $p_R = 1$ , and  $\gamma = 1.4$ . See the next figure for the results of 800 cells and 6400 cells.

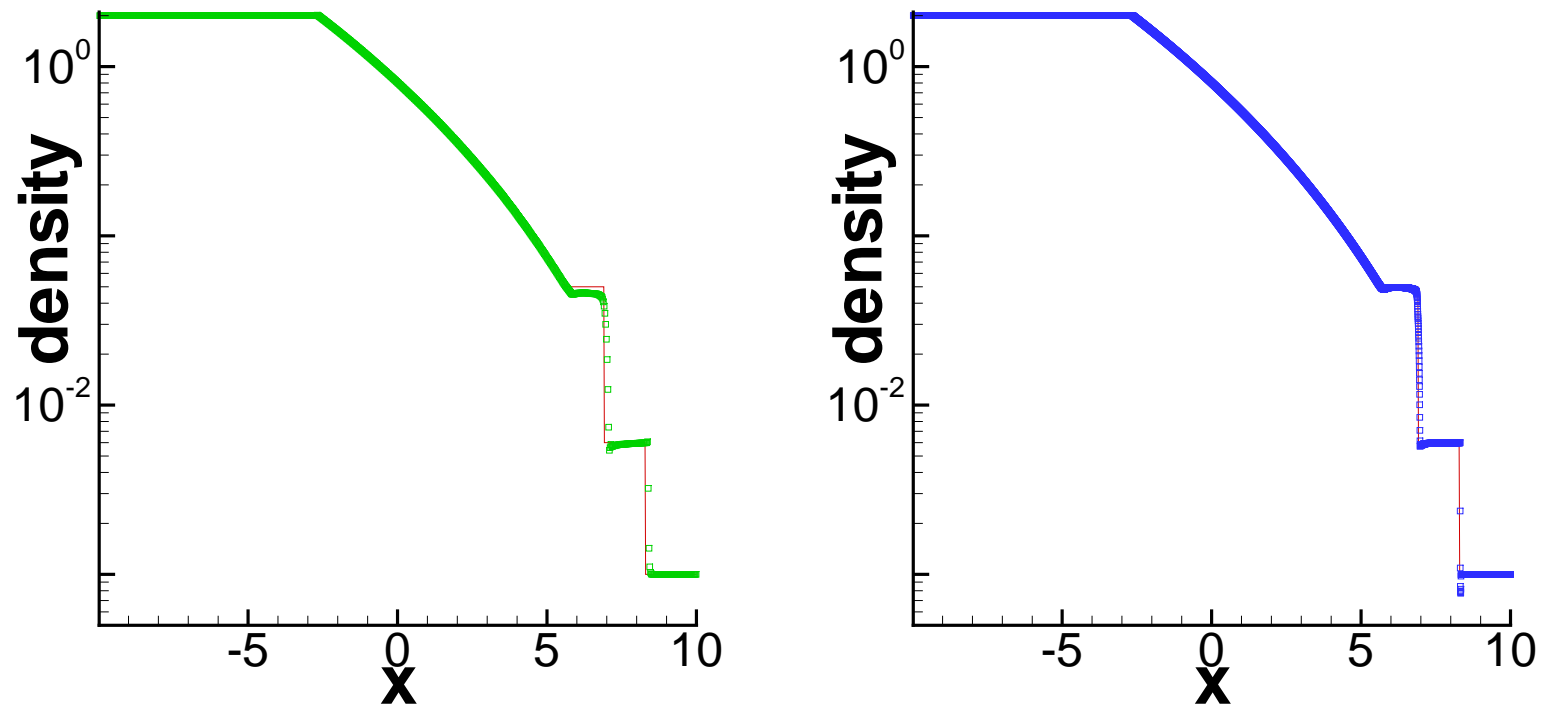


Figure 10: Leblanc problem.  $T = 0.0001$ . Left:  $N = 800$ . Right:  $N = 6400$ . The solid line is the exact solution. Symbols are numerical solutions.  $\Delta x = \frac{20}{N}$  with the positivity limiter. log-scale of density.

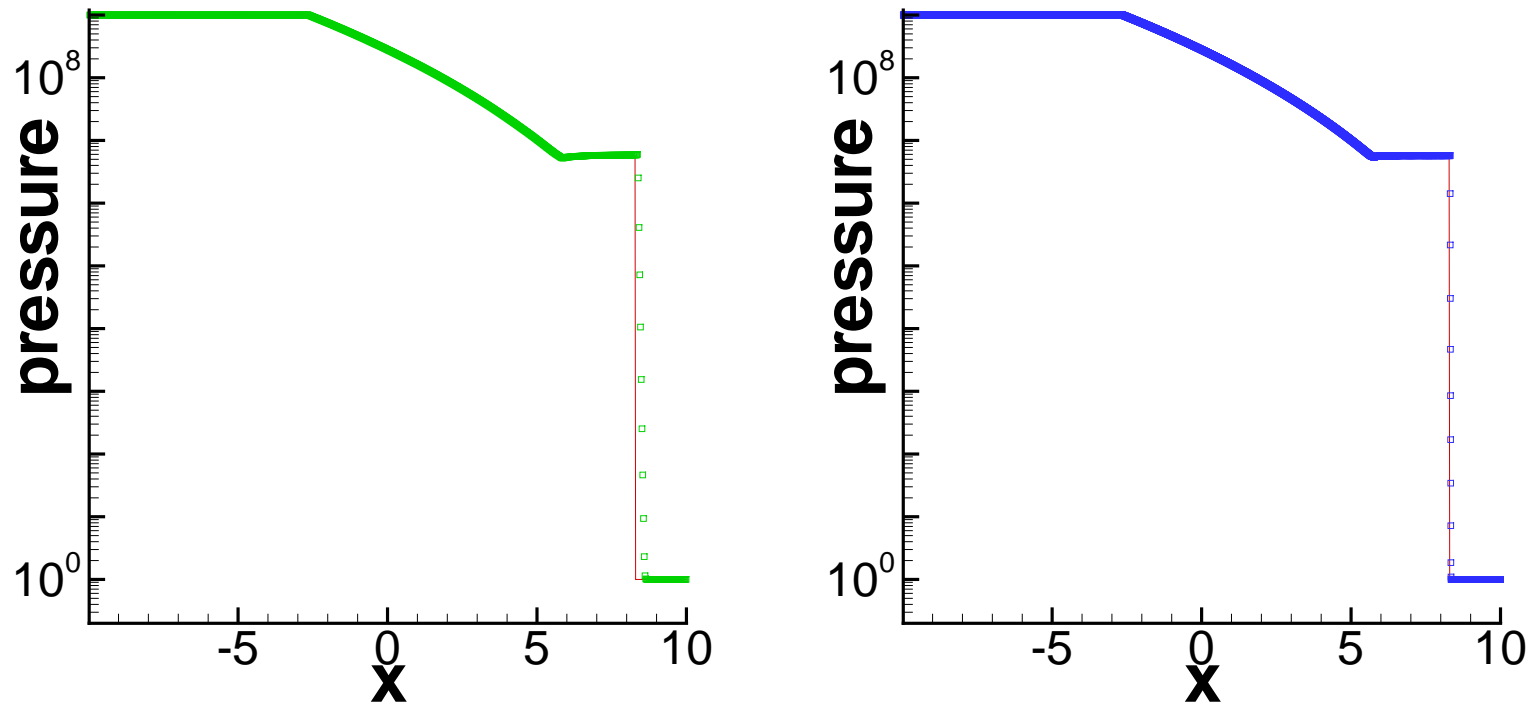


Figure 11: Leblanc problem.  $T = 0.0001$ . Left:  $N = 800$ . Right:  $N = 6400$ . The solid line is the exact solution. Symbols are numerical solutions.  $\Delta x = \frac{20}{N}$  with the positivity limiter. log-scale of pressure.

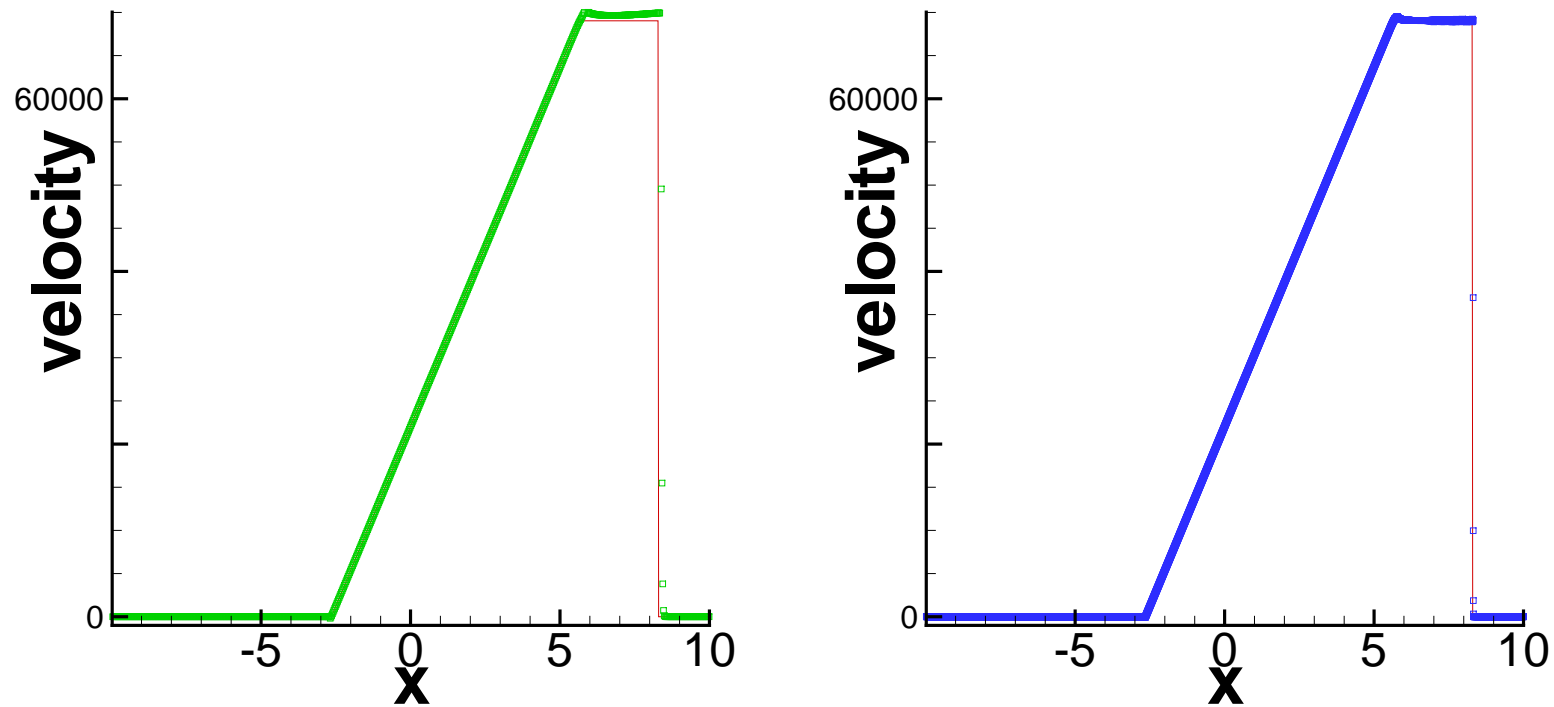


Figure 12: Leblanc problem.  $T = 0.0001$ . Left:  $N = 800$ . Right:  $N = 6400$ . The solid line is the exact solution. Symbols are numerical solutions.  $\Delta x = \frac{20}{N}$  with the positivity limiter. Velocity.

**Example 6.** To simulate the gas flows and shock wave patterns which are revealed by the Hubble Space Telescope images, one can implement theoretical models in a gas dynamics simulator. The two-dimensional model without radiative cooling is governed by the compressible Euler equations. The velocity of the gas flow is extremely high, and the Mach number could be hundreds or thousands. A big challenge for computation is, even for a state-of-the-art high order scheme, negative pressure could appear since the internal energy is very small compared to the huge kinetic energy ([Ha, Gardner, Gelb and Shu, JSC 2005](#)).

First, we compute a Mach 80 (i.e. the Mach number of the jet inflow is 80 with respect to the soundspeed in the jet gas) problem without the radiative cooling.

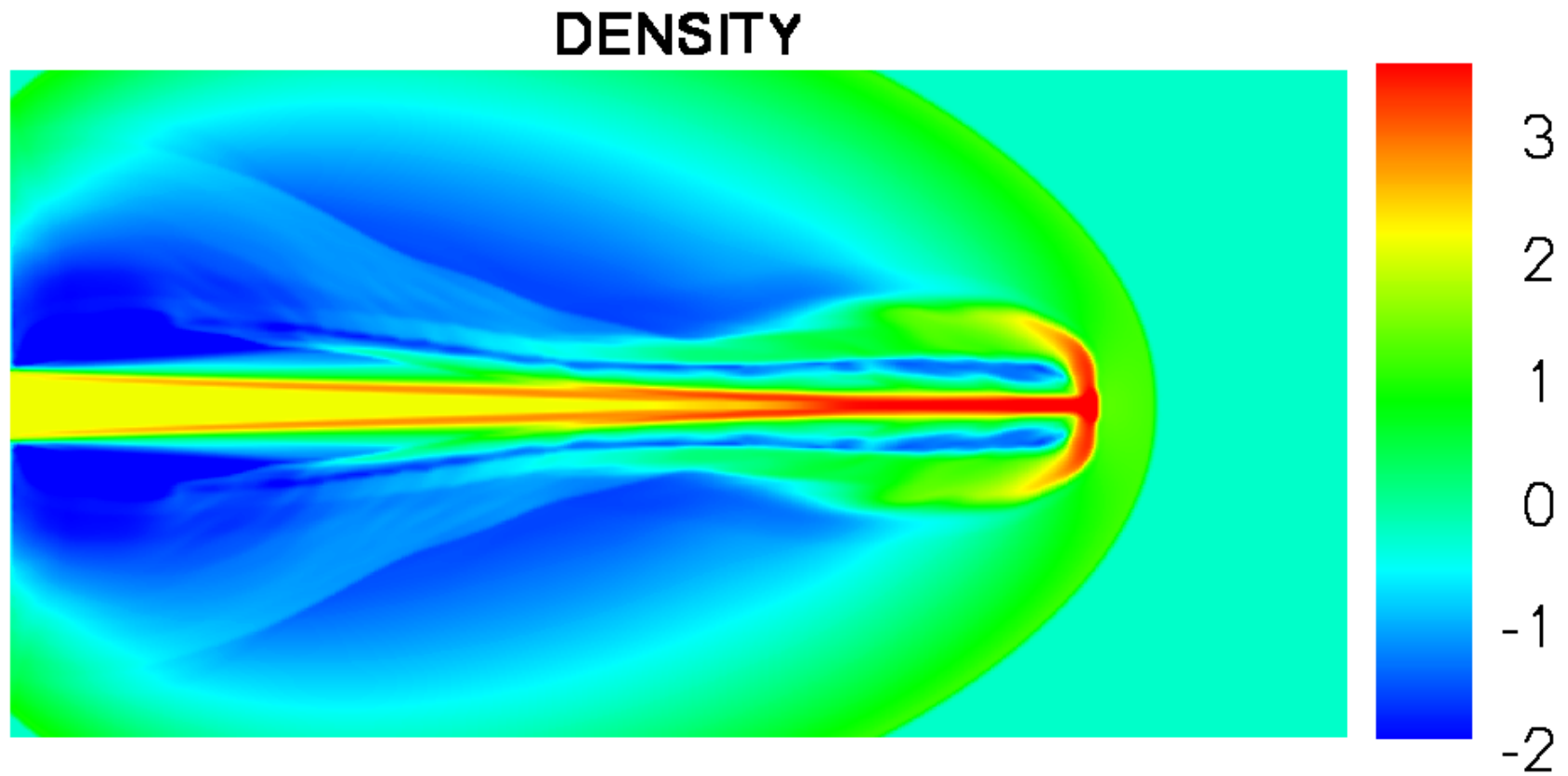


Figure 13: Simulation of Mach 80 jet without radiative cooling. Scales are logarithmic. Density.

Second, to demonstrate the robustness of our method, we compute a Mach 2000 problem. The domain is  $[0, 1] \times [0, 0.5]$ . The width of the jet is 0.1. The terminal time is 0.001. The speed of the jet is 800, which is around Mach 2100 with respect to the soundspeed in the jet gas. The computation is performed on a  $640 \times 320$  mesh. TVB limiter parameters are  $M_1 = M_2 = M_3 = M_4 = 100000000$ .

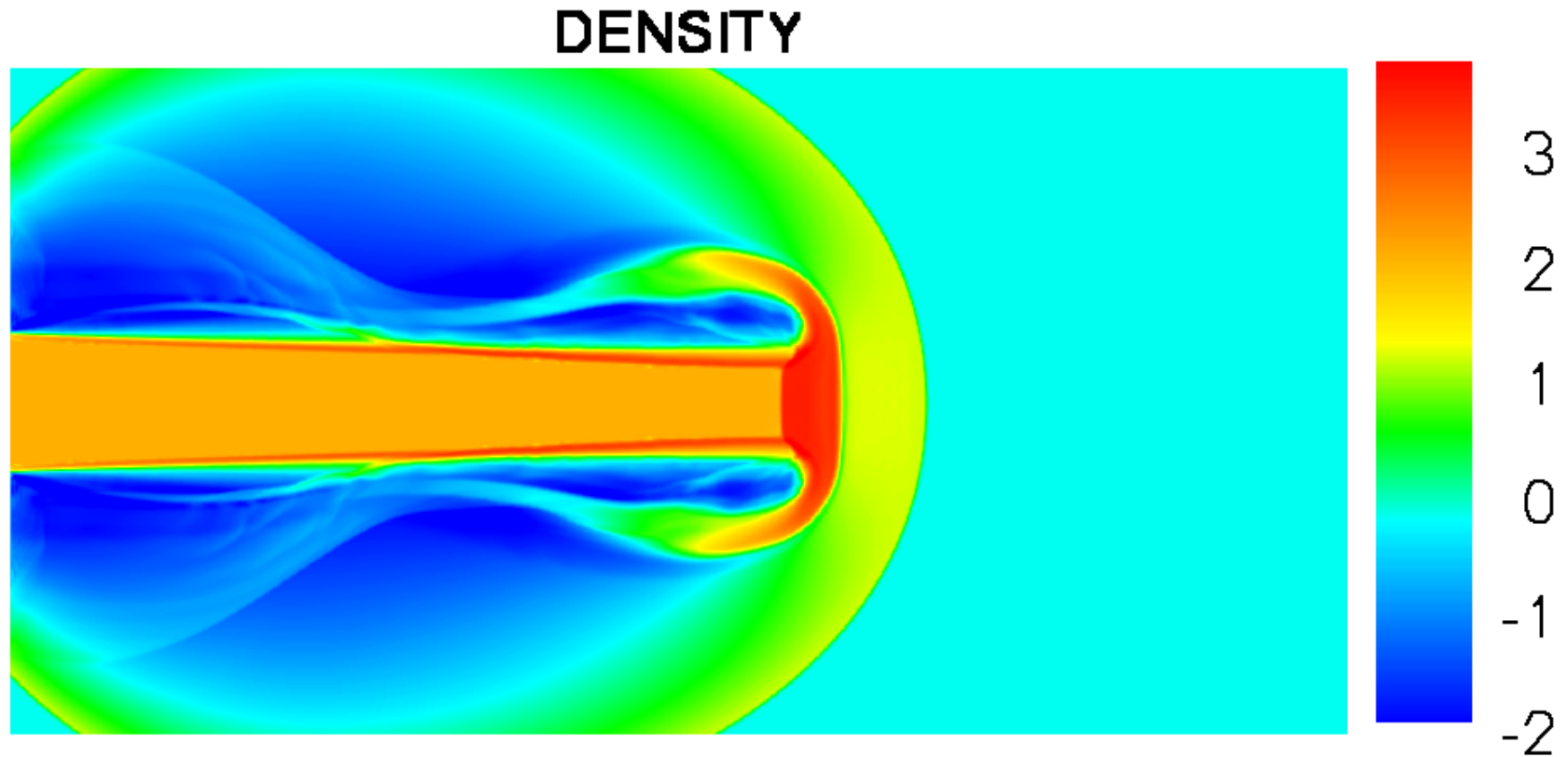


Figure 14: Simulation of Mach 2000 jet without radiative cooling. Scales are logarithmic. Density.



Lastly, we compute a Mach 80 (i.e. the Mach number of the jet inflow is 80 with respect to the soundspeed in the jet gas) problem with the radiative cooling to test the positivity-preserving property with the radiative cooling source term.

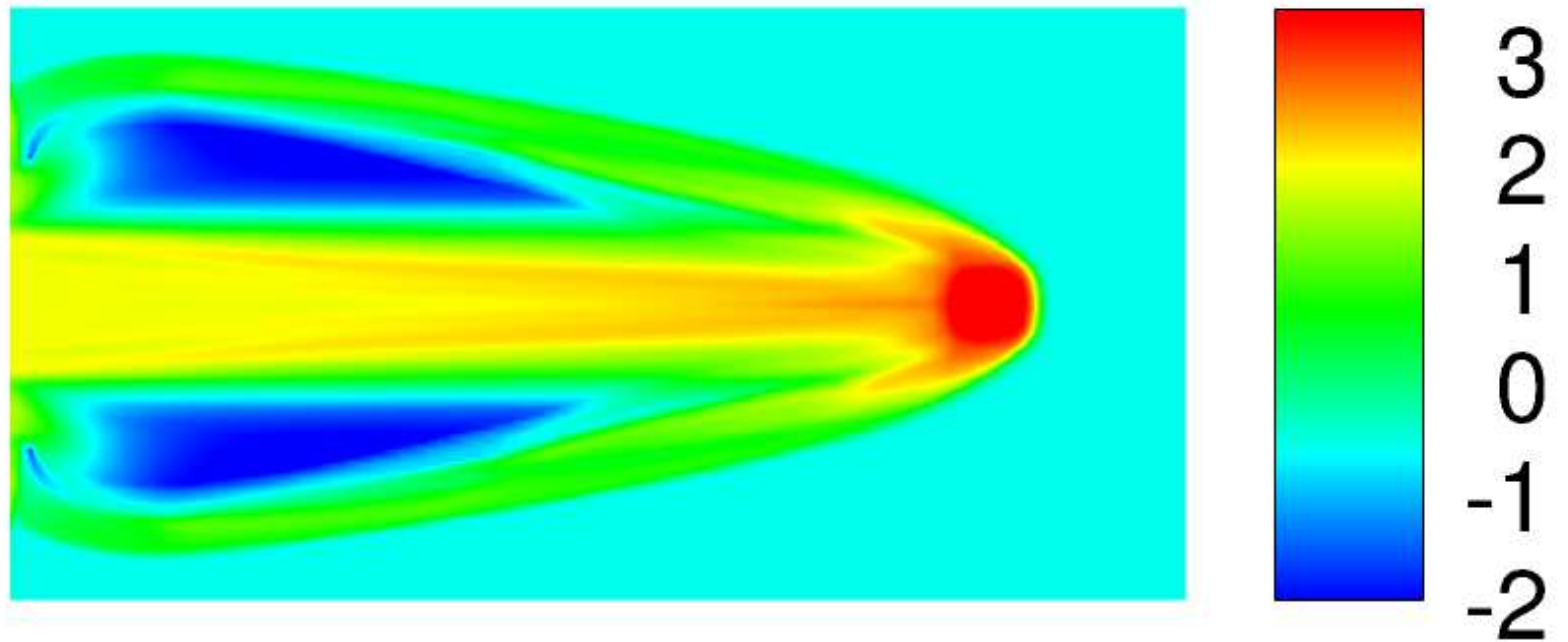


Figure 15: Simulation of Mach 80 jet with radiative cooling. The third order positivity-preserving RKDG scheme with the TVB limiter. Scales are logarithmic. Density.

**Example 7.** Shock diffraction problem. Shock passing a backward facing corner of  $135^\circ$ . It is easy to get negative density and/or pressure below the corner. This problem also involves mixed triangular / rectangular meshes for the DG method. The initial conditions are, if  $x < 1.5$  and  $y \geq 2$ ,  $(\rho, u, v, E, Y) = (11, 6.18, 0, 970, 1)$ ; otherwise,  $(\rho, u, v, E, Y) = (1, 0, 0, 55, 1)$ . The boundary conditions are reflective. The terminal time is  $t = 0.68$ .

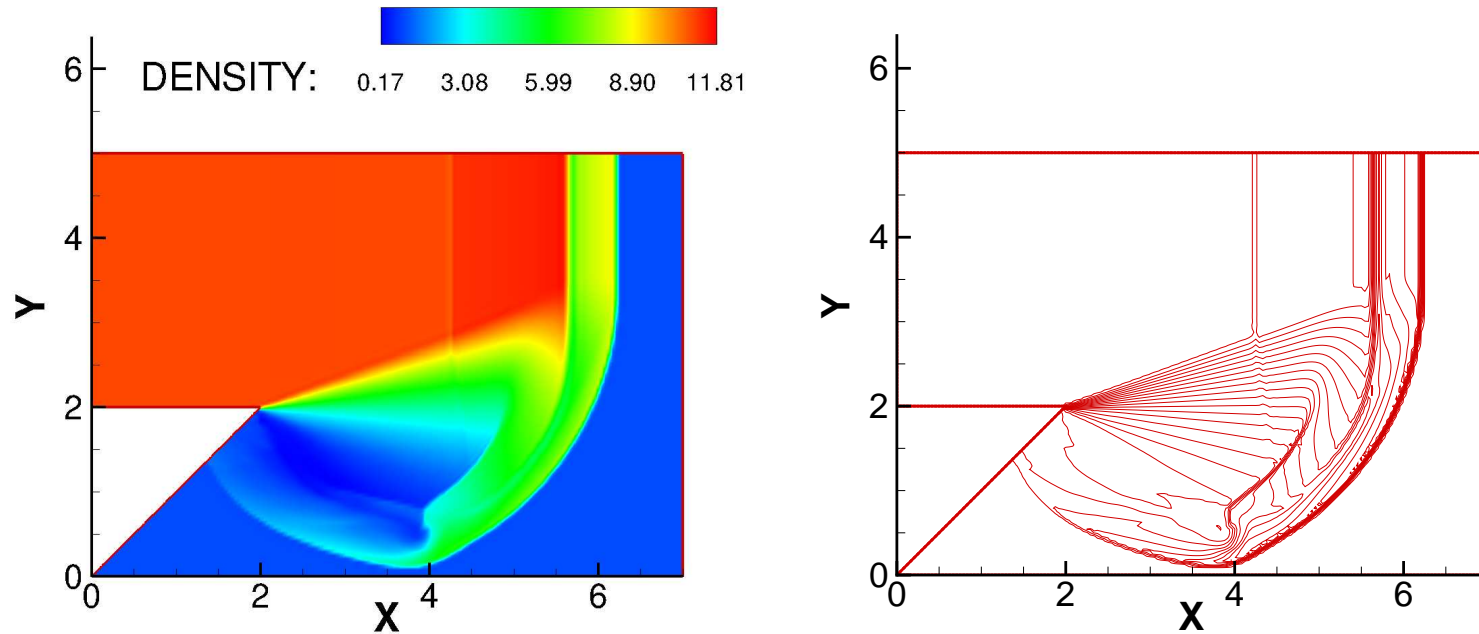


Figure 16: Density. Detonation diffraction at a  $135^\circ$  corner.

## Conclusions and future work

Topics not discussed: Bound-preserving convection-diffusion equations including Navier-Stokes equations

- Second or at most third order DG methods for general convection-diffusion equations ([Zhang, Zhang and Shu, JCP 2013](#); [Chen, Huang and Yan, JCP 2016](#))
- High order non-standard finite volume schemes ([Zhang, Liu and Shu, SISC 2012](#))
- High order DG or finite volume methods for Navier-Stokes equations ([Zhang, JCP 2017](#))

## Summary and future work:

- There is a general framework to obtain uniformly high order bound-preserving schemes for multi-dimensional nonlinear conservation laws and other hyperbolic equations including the radiative transfer equations.
- In the future we will design higher order bound-preserving DG schemes for other types of PDEs and other types of time discretizations.

THANK YOU!